JOURNAL OF CATALYSIS 28, 161–173 (1973)

Studies of a Triply Promoted Ammonia Synthesis Catalyst with an Electron Probe Microanalyzer

HONG-CHIU CHEN* AND ROBERT B. ANDERSON

Department of Chemical Engineering and Institute for Materials Research, McMaster University, Hamilton, Ontario, Canada

Received June 23, 1972

Electron probe studies of an iron ammonia synthesis catalyst promoted with Al_2O_3, CaO and K_2O are described. The catalyst was not homogeneous on a micrometer scale. A large portion of the structural and chemical promoters was sequestered by silica to form slag-like envelopes surrounding grains of magnetite which contained only small amounts of these promoters. Large cracks and holes associated with the envelopes provided a good ventilation system in the catalyst particles which facilitated the entry of hydrogen and removal of steam during reduction and the entry of hydrogen sulfide in the poisoning experiments. The reduction started at the periphery of a particle and proceeded from this point toward the center along the envelopes. However, some portions near the periphery remained unreduced while other portions in the interior were already reduced completely. At 25°C a small amount of hydrogen sulfide was adsorbed in the reduced magnetite grains throughout a particle. At 450°C large amounts of hydrogen sulfide were adsorbed near the periphery or at positions inside the particle where easy entry of H_2S was possible. In the portions near the periphery where adequate H_2S was available, FeS was formed.

INTRODUCTION

In a previous paper (*2*) the electron probe studies of an ammonia synthesis catalyst promoted with MgO and K_2O were reported. The present paper reports a similar examination of an ammonia synthesis catalyst promoted with Al_2O_3, CaO and K_2O, including the general morphology of the catalyst, the distribution of promoters, and the reduction and poisoning of catalyst particles.

Promoted fused magnetite has been the standard catalyst for the ammonia synthesis for a half century. These catalysts contain about 1% K_2O as a chemical promoter. Structural promoters are usually Al_2O_3, MgO, or Al_2O_3 + CaO, and generally total 3 to 4% by weight. Other nonreducible oxides are sometimes found in the catalyst; in some cases they are added and in other cases they are impurities in the magnetite. The literature of ammonia synthesis catalysis has been reviewed (*3–5*).

The degree of dispersion of the promoters in the magnetite is not fully understood; however, available data suggest that at least a fraction of structural promoters is present in the magnetite as spinels (*6–13, 16, 17*). Silica or potassium oxide usually do not enter the magnetite structure (*9, 13*). Optical microscopic examination of catalysts containing SiO_2, TiO_2, and ZrO_2 showed amorphous layers separating magnetite grains (*18*). Slag-like inclusions of a potassium–silica glass have been found in a promoted catalyst containing silica (*19*). In a triply promoted catalyst containing Al_2O_3, CaO, and K_2O, electron

* Taken in part from the doctoral thesis (*1*) of Hong-chiu Chen, Dept. of Chemical Engineering, McMaster University. Present address: Chemistry & Materials Science Division, Whiteshell Nuclear Research Establishment, Atomic Energy of Canada, Ltd., Pinawa, Manitoba.

microprobe pictures showed the presence of Al and Ca both in the magnetite grains and in the grain boundaries, but potassium was found only in the grain boundaries (*5*).

Preparations containing structural promoters are generally more difficult to reduce than pure Fe_3O_4, and the reduced catalysts have larger surface areas. The surface of the reduced catalyst contained larger fractions of structural promoters and alkali than are present in the catalyst (*14, 15*). In the reduction of an iron ammonia synthesis catalyst, magnetite is reduced directly to iron, and the external dimensions of the particle remain constant (*7, 20*). Rate data suggest that the reduced zone progresses, at least on a macroscale, uniformly inward from the external surface.

Hydrogen sulfide is a permanent poison for the ammonia synthesis catalysts. Promoted catalysts were reported to be more resistant to H_2S poisoning than the pure magnetite catalyst (*21*). H_2S (1 ppm) in the synthesis gases was enough to cause severe poisoning of a catalyst containing Al_2O_3 and K_2O (*22*) and a catalyst promoted with Al_2O_3, K_2O and CaO (*5*). The effects of preadsorbed sulfur compounds on the activity of a catalyst containing K_2O and MgO in Fischer-Tropsch synthesis has also been studied (*22*). Chemisorption studies with CO and CO_2 on promoted catalysts preadsorbed with H_2S showed that the surface covered by K_2O were preferentially poisoned compared with the iron surface in a catalyst containing K_2O and MgO; however, the reverse was observed in a catalyst promoted with K_2O and Al_2O_3 (*3*).

The electron probe microanalyzer provides nondestructive analyses for volumes of material the order of a few cubic micrometers, and thus it must be regarded as a "blunt" tool for examining some aspects of catalysts, especially where interesting features may be a hundredfold smaller than the resolution of the probe. This instrument has proved useful in examining Raney nickel alloys and in following their activation in aqueous alkali (*24*). The electron microprobe has also been used to obtain concentration profiles in impregnated catalysts (*1, 25, 26*).

Experimental Procedures

A 6- to 8-mesh sample of a commercial triply promoted ammonia synthesis catalyst containing in addition to magnetite K_2O, Al_2O_3, CaO and SiO_2, was used.

Figure 1 shows the apparatus for reducing and poisoning the catalyst. The system contains a reaction vessel, a gas chro-

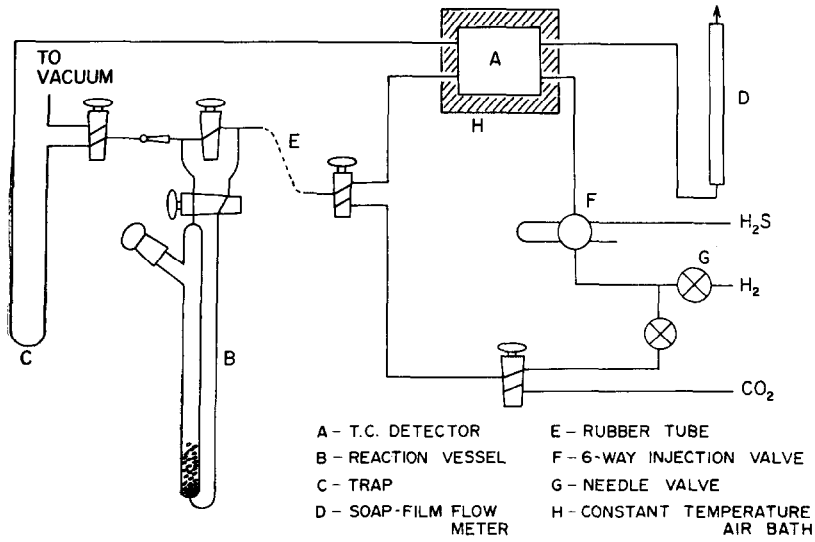

Fig. 1. The apparatus for reducing and poisoning catalysts.

matography gas injection valve and a thermal conductivity cell. The reaction vessel with a four-way stopcock (7) could be removed from the system for weighing on an analytical balance. The Gow-Mac thermal conductivity cell with the filament temperature at about 50°C was placed in an insulated box, and a Varian 6-way gas sampling valve with a sampling loop of 3.52 ml was used.

The catalyst was reduced in hydrogen in the reaction vessel at 450 ± 10°C. The extent of reduction was determined from the weight loss. For studies of the reduced catalysts, the sample was reduced 50%. Samples for poisoning studies were reduced about 90%. Conditions of the reduction and poisoning experiments are summarized in Table 1.

In the poisoning experiments pulses of H_2S in hydrogen were passed over reduced catalyst at 25 or 450°C, and the flow rate of hydrogen was 39 ml/min. A pulse of H_2S passes first through one side of the thermal conductivity cell, over the catalyst, and through the other side of the thermal conductivity cell. From the ratio of the recorded peak areas the fraction of H_2S adsorbed by the catalyst was measured and from the volume and number of pulses the sulfur retained by the catalyst was calculated.

For poisoning at 25°C about 5 g of catalyst were used. At the beginning a large fraction of the pulse was retained by the particles. Near the end of the poisoning experiment only a small fraction of the pulse was retained. The fraction of the H_2S pulse adsorbed by the particles decreases from 1 to 0.16 in 22 pulses. For poisoning at 450°C about 7 g of catalysts were used and the fraction of each H_2S pulse retained by the particles decreased from 1 to 0.34 in 50 pulses.

For Sample C the poisoning was performed at 25°C, and 7.46 mg H_2S/g reduced catalyst were retained from 22 pulses. The sample was heated in hydrogen at 500°C for 1 hr in the reaction vessel. For Sample D the catalyst was poisoned at 450°C until 16.81 mg H_2S/g reduced catalyst was retained from 50 pulses. These quantities were the net amounts of H_2S retained by the particles excluding the amounts retained by the glass and rubber tubings. However, these values are average sulfur concentrations in the entire sample, and differences in sulfur content may be expected from the inlet to outlet portions of the sample. Only a few particles were chosen at random for examination.

At the end of reduction or poisoning experiments the sample was cooled in hydrogen to room temperature, and CO_2 was flowed over the sample. With CO_2 flowing over the sample, the reaction vessel was detached and the glass joint on the filling tube of the reaction vessel was removed. The catalyst was then poured from the reaction vessel in flowing CO_2 into a bottle containing benzene. This procedure prevented contamination of the sample by air.

The particles wet with benzene were then mounted in Bakelite. The sample was

TABLE 1

CONDITIONS FOR REDUCING AND POISONING THE TRIPLY PROMOTED CATALYST

	Reduction				Poisoning with H_2S		
Sample	Temp (°C)	Hourly space velocity of H_2	Time (hr)	Extent %	Temp (°C)	Amount (mg H_2S/ g reduced cat)	Heat treatment
A	450	1000	18	50	—	—	—
C	450	1000	86	89	25	7.46	500°C in H_2 for 1 hr
D	450	2000	60	88	450	16.81	—
E	450	1000	86	89	25	7.46	—

first polished using silicon carbide paper with water as the lubricant. After the polishing the sample was washed with water and then cleaned with petroleum ether. The sample was further polished by 5-μm diamond paste followed by 1-μm diamond paste on polishing wheels with kerosene as the lubricant. After each polishing the sample was cleaned with petroleum ether. The polished sample was coated with a layer of evaporated carbon to ensure adequate electrical conductivity for probe analysis. Extensive oxidation of the reduced catalysts apparently did not occur in any of the steps of the preparation. Particles of the raw catalyst were also mounted in Bakelite and polished as described above.

Optical pictures of the cross-sections of the particles were made with a Zeiss Ultraphot II microscope.

Experimental Results

Figures 2 to 4 present optical micrographs of cross-sections of unreduced and partly reduced (about 50%, sample A) particles, and Fig. 5 compares electron probe results with the optical micrograph for the reduced catalyst. In Fig. 5 each micrograph designated with the name of an element is the image of the X-ray quanta of that element from the sample. The density of the white spots is a measure of the X-ray intensity and the concentration of the element, thus providing a semiquantitative analysis of the cross-section. The micrograph designated as "Electron" is the specimen current image. In a region containing lighter elements, fewer electrons are backscattered and more pass through the sample giving a bright specimen current image. However, less specimen current passes through the region containing heavier elements and gives rise to a darker image.

A dendritic pattern is the principal structural feature of this catalyst. The cross-sections also contain pits, particularly in unreduced portions, and large fissures and holes (black areas). Some of these features are characteristic of the catalyst such as the pitted areas in the polished unreduced catalyst. The large holes and fissures result from polishing. As shown in Fig. 5 the dendritic structure is composed of grains containing principally iron, enveloped by a slag-like material containing most of the promoters and silica.

In Figs. 2C, D and 4B, white areas are reduced and the gray pitted areas not reduced. The specimen shown on top of Fig. 3 was coated with carbon, and here the dark smooth areas were reduced and the gray pitted material not reduced. By point-counting the unreduced areas were shown to have the same iron concentration as the grains in the unreduced catalyst, and the

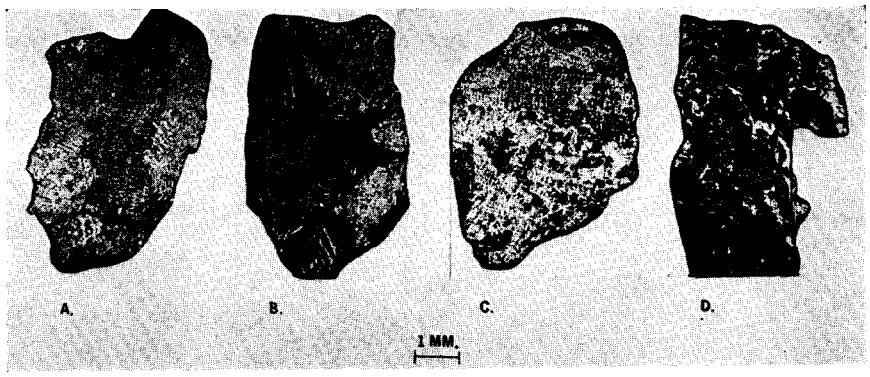

Fig. 2. Optical pictures of catalyst particles; (A) and (B): unreduced, (C) and (D): reduced. The envelopes contain large amounts of promoters and silica. The area between the envelopes, the grains, are principally magnetite or iron. In (C) and (D) the light areas are reduced while the grey pitted areas are not reduced.

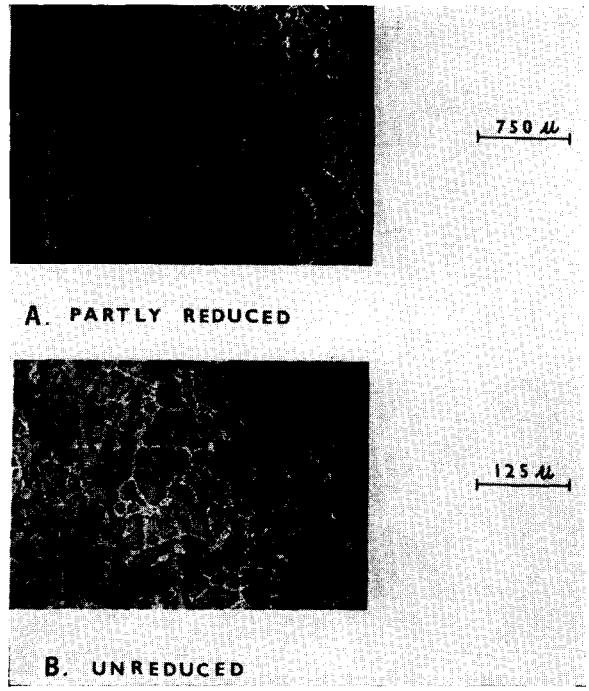

FIG. 3A. A portion near the periphery of a reduced particle, with the dark area reduced and the grey pitted area unreduced. The reduction starts at the periphery and proceeds inward along the envelopes. (B) A portion of an unreduced particle.

reduced areas an iron content of about 90%, as described below.

We may infer from the micrographs of the partly reduced catalyst that the reduction starts at the periphery and proceeds inwards along the slag-like envelopes, and particles containing many of these structures reduce more rapidly, e.g., compare Fig. 2C, which is nearly completely reduced, with 2D.

The cross-sections of the unreduced particles shown in Fig. 2A and B were not coated with carbon, and thus show the envelopes darker than the grains. Those

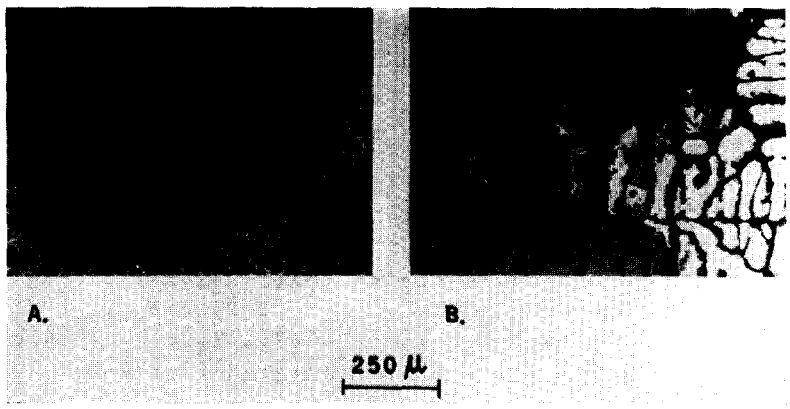

FIG. 4A. Unreduced and (B) reduced. Grains of magnetite are surrounded by envelopes. The sample in (A) is coated with carbon but the sample in (B) is not. In (B) the white areas are reduced, the grey areas are unreduced and the black areas are envelopes.

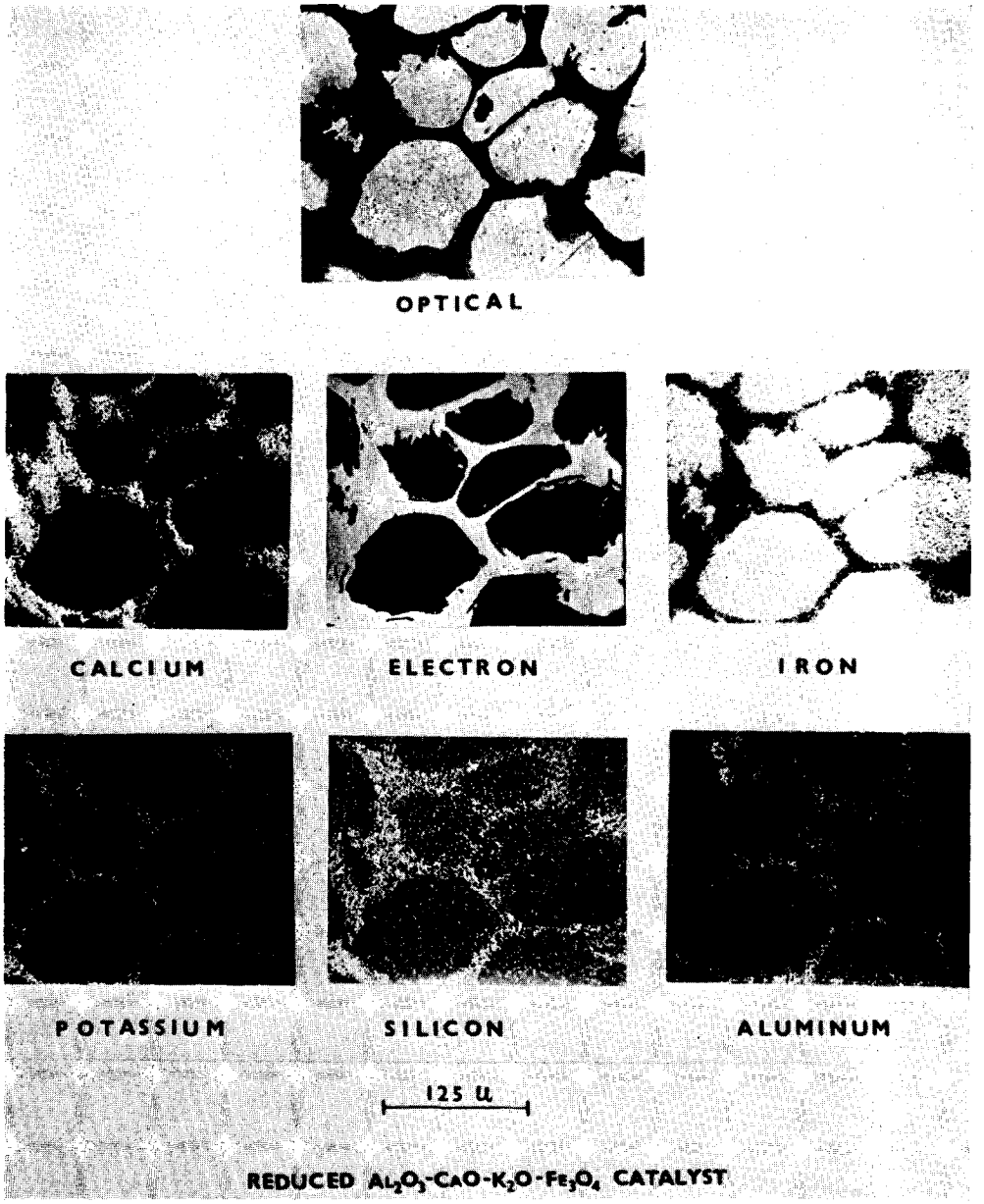

FIG. 5. Probe examination of a reduced particle. Each picture designated with an element name is an X-ray picture with the number of white spots proportional to the concentration of the element. The picture designated with "Electron" is the specimen current image. The grains contain large amounts of Fe but small amounts of promoters and silica; in the envelopes the compositions are reversed.

shown on bottom of Figs. 3 and 4A were coated with carbon and the grains are darker than the envelopes.

More completely reduced catalysts (about 90%) were treated with pulses of H_2S in H_2; in one case at 25°C and the sample was subsequently heated in H_2 at 500°C. In the second case the H_2S treatment was done at 450°C.

Figure 6 shows the micrograph and its

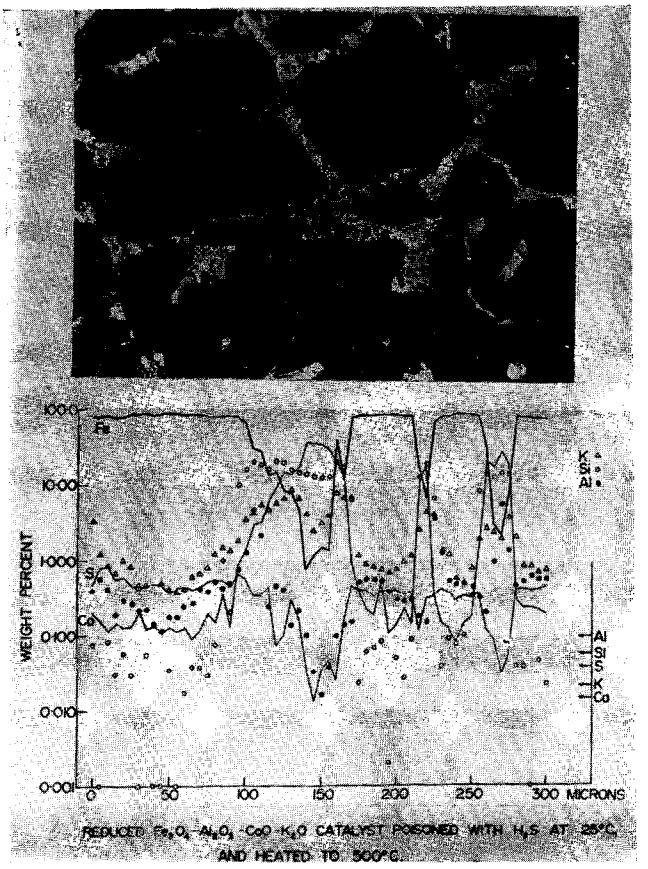

FIG. 6. Point-counting results at 5-μm intervals along the dotted line in the picture.

corresponding concentration diagram on a portion in the interior of a particle of Sample C (reduced, H_2S-treated at room temperature and heated to 500°C). Point-countings were performed at 5-μm intervals along the dotted line in the micrograph.

The concentrations of elements are plotted on a logarithmic vertical scale as a function of linear distance corresponding to the micrograph. The variation of iron content is indicated by a thick line while those of calcium and sulfur are by thin lines. The concentrations of potassium, silicon and aluminum are indicated by different symbols. Also shown on the concentration graph as arrows are the limits of uncertainty and detectability of elements according to the criterion described elsewhere (*2*). Concentrations below the limit of uncertainty and detectability may be due to the random emission of X-rays, and even the presence of the element is uncertain. However, concentrations above the limit of uncertainty and detectability indicate the existence of the elements with 95% confidence level.

The iron concentration is high and uniform in the grains with an average value of 86.7%. The iron content in the slag-like envelopes is lower and nonuniform. The concentration of the silicon is low in the grains but high in the envelopes with the concentration change from the grains to the envelopes being more than one hundredfold.

The concentrations of calcium, aluminum and potassium are also low in the grains but high in the envelopes. Except for cal-

cium, the concentrations change less abruptly than silicon from the grains to the envelopes. Promoter contents higher than their limits of uncertainty and detectability are found in the grains. Their existence in the grains can be assured, but the silicon with its overall concentration much lower than the promoters shows values higher than its limit of uncertainty and detectability only at a few points in the grains.

The sulfur content varies similarly to the iron curve, being higher in the grains than in the slag-like envelopes. Thus, sulfur is adsorbed by reduced iron. At room temperature, however, the rate of adsorption of H_2S must be slow, because the sulfur was distributed fairly uniformly through the particle. A uniform distribution of sulfur was also obtained for a reduced sample treated with H_2S at 25°C but without the subsequent heat treatment at 500°C (Sample E).

Figure 7 shows the cross-section of a complete particle of Sample D (reduced, H_2S-treated at 450°C). In the probe analysis this particle was moved at constant speed under the electron beam along the dotted lines from A to B and from C to D and the variations in X-ray intensities of iron and sulfur were recorded. The horizontal chart shows the variations of Fe and S X-rays along AB, while the vertical chart shows those along CD. In both charts the

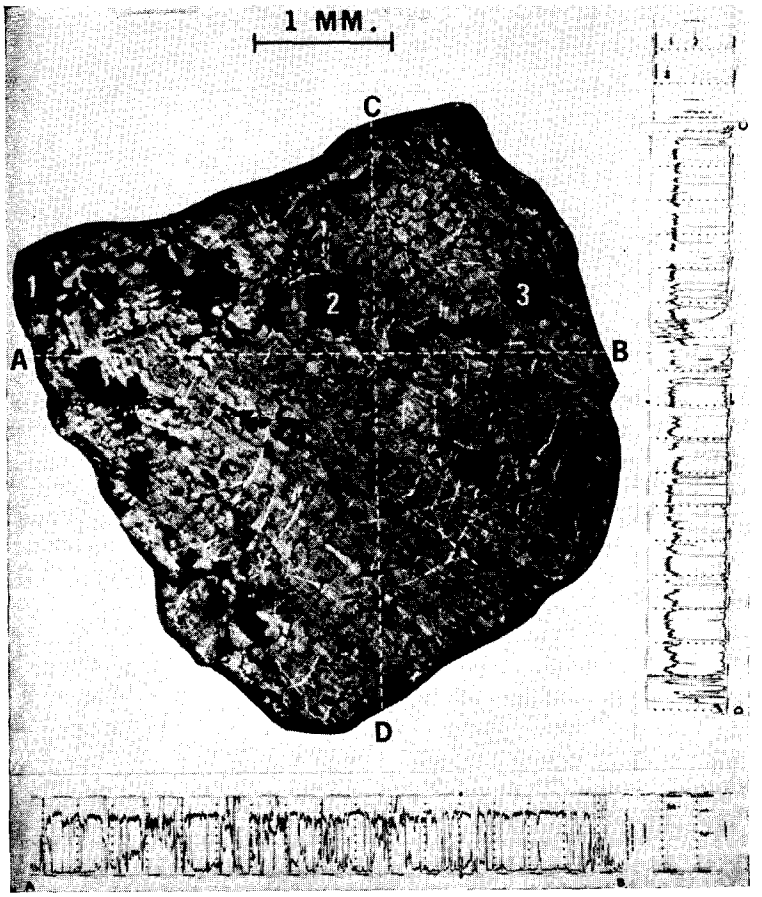

FIG. 7. Fe and S X-ray recordings across the particle from A to B and from C to D along the dotted lines. Square areas 1, 2 and 3 were scanned by the electron beam with results in Fig. 8. High S content was found near the periphery or the holes.

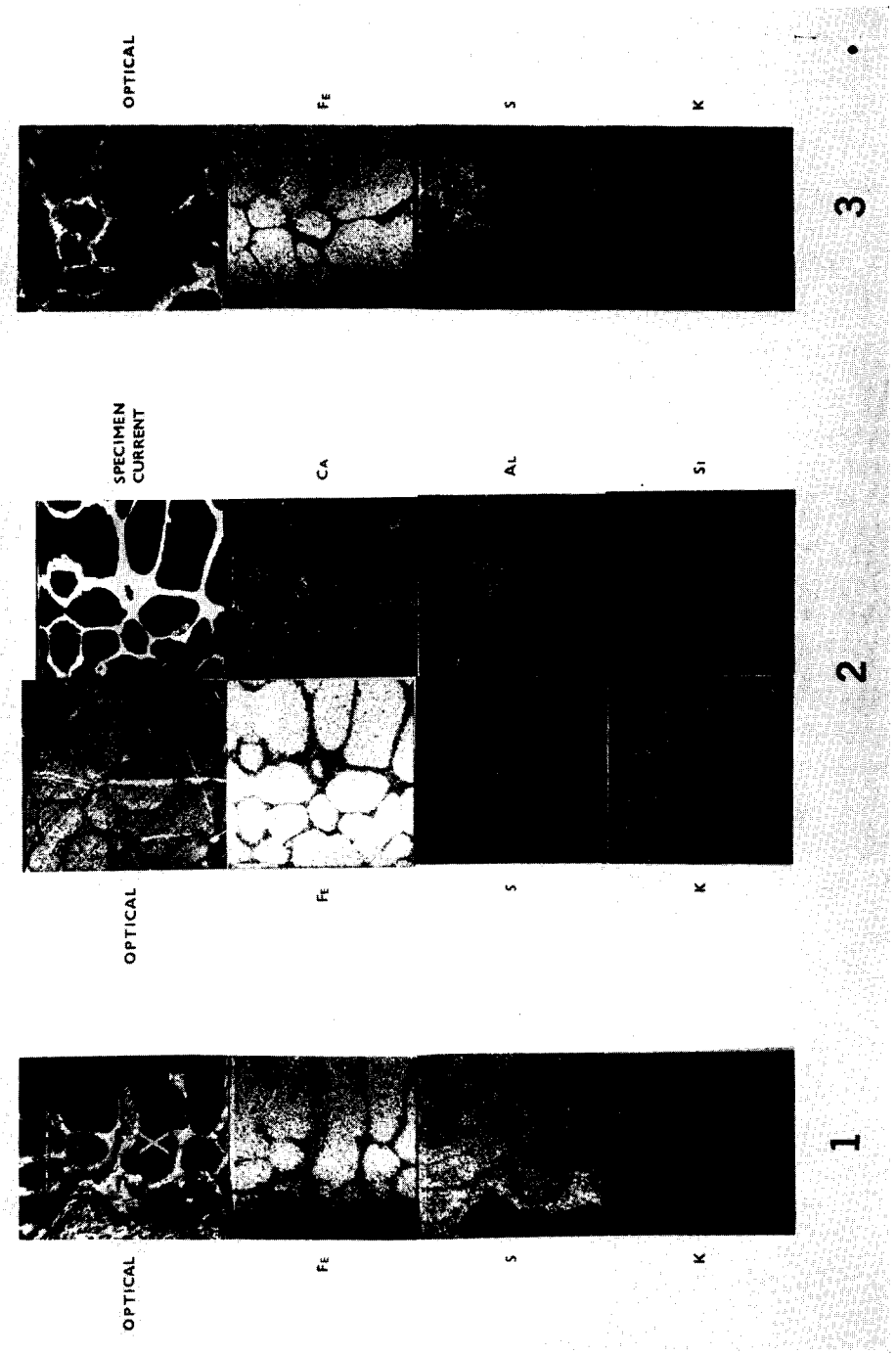

FIG. 8. Probe examination of the square areas 1, 2 and 3 in Fig. 7.

higher curve is for Fe and the lower curve is for S. Concentration profiles on a part of the particle is shown on a larger scale in Fig. 9.

Except at a few locations the S X-ray intensity is usually low. With reference to the picture of the particle, the locations with high S X-ray intensity are either near the periphery of the particle or situated close to cracks or holes. One obvious instance is at the intersection of AB and CD, which is adjacent to a large hole. Here high S X-ray intensities are shown on both charts.

Three square areas 300 × 300 μm were chosen for an area-scan by the electron beam. They are designated as 1, 2 and 3 in Fig. 7, and can be identified by the dark contamination deposit. The optical picture, specimen current image and X-ray pictures on these areas are shown in Fig. 8 designated 1, 2 and 3, respectively.

In the optical picture of Fig. 8-1 a crack extends from the boundary of the particle into the interior along the envelopes above the grain (X). The Fe X-ray picture shows the contour of the grains and the boundary of the particle clearly. In the grains near the boundary of the particle the iron content is lower, because this portion has a large sulfur content as shown by the S X-ray picture. A large sulfur content is also found in the upper portion of the grain (X). The crack near this grain provides easy entry of H_2S and causes deposition of sulfur in the portion of the grain near the crack. Little sulfur is found in the slag-like envelopes where the potassium content is large.

As shown by the S X-ray picture of Fig. 8-2, low sulfur concentration is found in the area 2 of Fig. 7 which is in the interior of the particle. The specimen current image and the X-ray pictures show the sequestering of the promoters and silicon from the grains.

From the S X-ray picture in Fig. 8-3, a large amount of sulfur is found in the grains at the right side of this area, which is near the periphery of the particle. High sulfur content is also found at the lower left corner of this area which is situated close to a large hole as shown in Fig. 7.

Point-countings were done in the area (1) of Fig. 7 with results shown in Fig. 9. The analyses were made at 5-μm intervals along the dotted line 0 to F shown in the micrograph. A crack extends from the boundary of the particle through the envelopes to a hole shown at the right side of the micrograph. Between 0 and A the crack gives rise to inaccurate X-ray readings.

The iron concentration is highest in EF, lower in CD and lowest in AB. The variation of the sulfur concentration is just the reverse, being highest in AB, lower in CD and lowest in EF. In the envelopes at BC and DE both the iron and sulfur contents are low. The atomic ratio of sulfur to iron equals 1 in AB and is smaller in CD and EF. Apparently, in AB where adequate H_2S is available, FeS is formed. The sulfur content in the iron-rich grains decreases from the boundary of the particle toward the interior. A minimum value is reached at a point 200 μm away from the boundary. The sulfur content then increases toward F. The higher sulfur content in this portion of the grain is caused by the easy entry of H_2S through the crack and the hole to this portion of the particle.

At 450°C the chemisorption of H_2S was sufficiently rapid and strong that at least most of the sulfur is found near the periphery of the particle or near cracks or holes.

Concentrations of the promoters and silicon higher than their limits of uncertainty and detectability are found in the grains. Much higher concentrations of these elements are observed in the envelopes.

During the measurement of the potassium X-ray peak and its background intensities in Fig. 9, the probe current drifted from 150 nA to 185 nA. The background intensity which was measured last when the probe current was at 185 nA gave rise to lower net X-ray intensity, yielding lower values for potassium.

The average concentrations of promoters, iron and silicon in the grains and the envelopes of Samples C, D and E are shown in Table 2. For Samples C and E the concentrations in the grains are the average values of the point-counting results in the grains traversed by the probe, while for

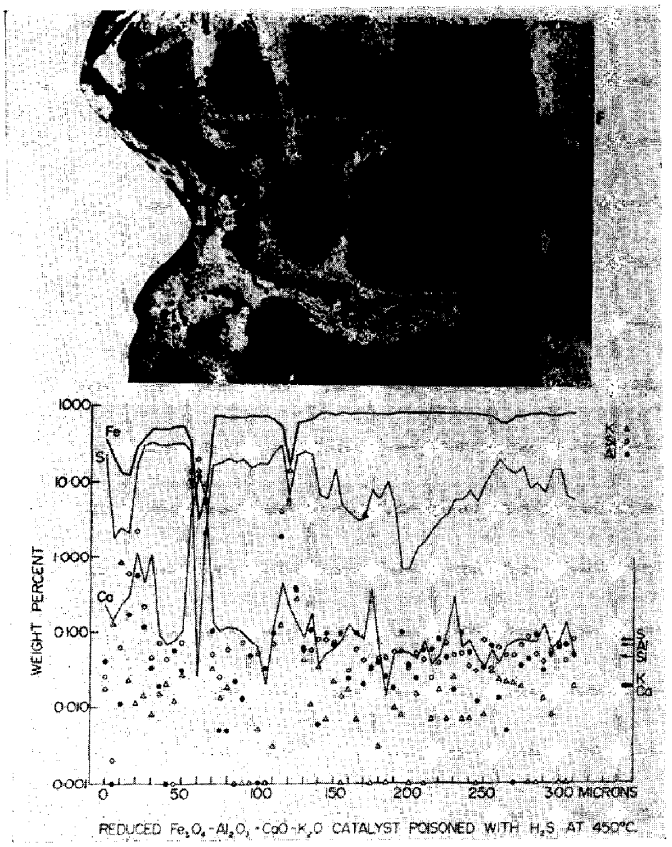

FIG. 9. Point-counting results at 5-μm intervals along the dotted line 0F.

Sample D, the concentrations are the average values in grain EF of Fig. 9.

The X-ray source in probe analysis covers a volume of a few cubic micrometers. Since the envelopes are usually narrow, the point-counting results in the envelopes at locations near the grains are often influenced by the composition of the

TABLE 2

AVERAGE CONCENTRATIONS ON SULFUR-FREE BASIS OF PROMOTERS, IRON AND SILICON IN THE GRAINS AND THE ENVELOPES

		Wt % in					
		Grains[a]			Envelopes[b]		
Element	Sample:	C	D[c]	E	C	D	E
Al		0.44	0.07	0.18	0.13	8.90	0.68
K		0.92	—	0.68	4.36	14.7	2.25
Ca		0.23	0.10	0.24	28.0	6.08	35.5
Fe		87.1	87.5	91.0	3.96	10.4	5.55
Si		—[d]	—[d]	—[d]	16.5	13.0	13.0

[a] Average weight percents in the grains.

[b] Average values of the weight percents at points in the envelopes with lowest iron content.

[c] Average values in grain EF of Fig. 9.

[d] Below limit of detection at most locations, i.e., less than about 0.05%.

grains. The concentrations in the envelopes in Table 2 are the average values of the locations with lowest iron content.

Discussion

The triply promoted ammonia synthesis catalyst has been shown to be a nonuniform material on a scale of micrometers. There are two kinds of structure in the unreduced catalyst: the grains and the slag-like envelopes. The grains are magnetite containing detectable amounts of the promoters but in much smaller concentrations than their overall contents in the catalyst. The envelopes contain a small amount of iron and large amounts of the promoters and silicon, and the concentrations of these elements are not uniform. The enveloping materials are mixed oxides of the promoters and silica that are formed in the initial fusion of the catalyst and probably have lower melting points than the magnetite grains. On cooling the magnetite grains containing dissolved promoters solidify first. The still molten low melting mixed oxides are "squeezed" around the solid magnetite grains and solidify as the slag-like envelopes surrounding the magnetite grains.

Reduction removes oxygen from the magnetite grains. The reduction starts at the periphery of a particle, and proceeds inward along the envelopes. Some portions of the particle near the periphery remain unreduced while other portions in the interior are already reduced completely. Apparently, cracks or large pores exist in the envelopes and provide routes of entry for hydrogen and escape of steam during the reduction.

From nitrogen adsorption at 77°K, the surface area of this catalyst after complete reduction at 450°C was 16 m^2/g Fe. By assuming the iron crystallites to be spherical and the surface area to be the sum of their outside surfaces, the average radius of the iron crystallites was calculated to be 240 Å. From X-ray line broadening experiments of a reduced catalyst promoted with K_2O, Al_2O_3 and CaO, the radius of the iron crystallites was reported to be 180 Å (*5*). The volume of the X-ray source in a sample is a few cubic micrometers, and thus contains thousands of these iron crystallites. The average promoter content in the grains as shown in Table 2 is the overall amount of each promoter in the X-ray source. No information is provided by the probe analysis regarding whether the promoters cover the surface of the iron crystallites.

However, if the promoters are assumed to cover the surface of the iron crystallites in monolayer the fraction of the iron surface covered by each promoter can be estimated. By using the values of the promoter content in the grains of Sample E in Table 2 and the cross-sectional molecular areas of close packed molecules (*28*), the fraction of the surface area covered by Al_2O_3, K_2O and CaO are 17.8, 64.9 and 25.4%, respectively. This calculation shows that only trace amounts of promoters are enough to cover a large fraction of the surface if dispersed molecularly on the surface. Chemisorption of CO on a reduced catalyst promoted with K_2O, Al_2O_3 and CaO indicated that 88 to 93% of the iron surface was covered by promoters (*5*).

The distribution of the promoters in the grains and envelopes varied widely for different particles as shown in Table 2, but the concentrations of promoters and silica were usually substantially larger in the envelopes than in the grains. In the grains, the contents of potassium, aluminum and calcium are higher than their limits of detection. Nielsen (*5*) observed a similar structure of grains and envelopes in a triply promoted catalyst; however, potassium was not found in the grains. The iron content of the grains varied from 87 to 91% (on a sulfur-free basis); these values seem reasonable for samples that were reduced only 89%.

H_2S reacts with the reduced magnetite grains rather than the envelopes at room and elevated temperatures. At room temperature the rate of adsorption of H_2S is slow, giving rise to a uniform distribution of sulfur through the particle. For poisoning at 450°C the sulfur content decreases from the periphery of a particle toward the center. At positions inside the particle

where easy entry of H_2S is possible, high sulfur content is observed. FeS is formed in the portion near the periphery of a particle.

In a doubly promoted catalyst (*2*) containing as promoters and impurities, MgO, K_2O, Cr_2O_3 and SiO_2, about 4% Mg was found in principal iron component. This catalyst had a minor iron component with a banded structure having alternating stripes of high (11%) and low (2%) Mg. Silica occurred in inclusions rather than as envelopes and all of the potassium was associated with the silica. Magnesium was usually not found in the silica and the amount of silica in the iron-rich components was usually below the limit of detectability. Reduction of the doubly promoted catalyst proceeded inward from the periphery of the particle, the reduced zone moving more rapidly inward in portions containing the lower concentration of magnesia. Thus, there are major differences in the structure of the two catalysts and the catalysts do not reduce in the same way.

References

1. Chen, H. C., PhD thesis, Department of Chemical Engineering, McMaster University, 1972.
2. Chen, H. C., and Anderson, R. B., *J. Colloid Interface Sci.* **38**, 535 (1972).
3. Frankenburg, W. G., *in* "Catalysis" (P. H. Emmett, Ed.), Vol. 3, pp. 171–263. Reinhold, New York, 1955.
4. Bokhoven, C., Van Heerden, C., Westrik, R., and Zwietering, P., *in* "Catalysis" (P. H. Emmett, Ed.), Vol. 3, pp. 265–348. Reinhold, New York, 1955.
5. Nielsen, A., "An Investigation on Promoted Iron Catalysts for the Synthesis of Ammonia," 3rd ed., pp. 264. Jul. Gjellerupups Forlag, Copenhagen, 1968.
6. Brill, R., *Z. Elektrochem.* **38**, 669 (1932).
7. Shultz, J. F., Hofer, L. J. E., Cohn, E. M., Stein, K. C., and Anderson, R. B., *U. S. Bur. Mines, Bull.* **578**, 139 (1959).
8. Wyckoff, R. W. G., and Crittenden, E. D., *J. Amer. Chem. Soc.* **47**, 2866 (1925).
9. Wilchinsky, Z. W., *Anal. Chem.* **21**, 1188 (1949).
10. Uchida, H., Terao, I., Ogawa, K., and Oba, M., *Bull. Chem. Soc. Jap.* **37**, 1508 (1964).
11. Burdese, A., and Brisi, C., *Ric. Sci.* **22**, 1564 (1952).
12. Vervey, E. J. M., Braun, P. B., Gorter, E. W., Romeyn, F. C., and Van Santen, J. H., *Z. Physik. Chem.* **198**, 6 (1951).
13. Dry, M. E., and Ferreira, L. C., *J. Catal.* **7**, 353 (1967).
14. Emmett, P. H., and Brunauer, S., *J. Amer. Chem. Soc.* **59**, 310 (1937); **62**, 1732 (1940).
15. Bayer, J., Stein, K. C., Hofer, L. J. E., and Anderson, R. B., *J. Catal.* **3**, 145 (1964).
16. Maxwell, L. R., Smart, J. S., and Brunauer, S., *J. Chem. Phys.* **19**, 303 (1951).
17. Love, K. S., and Brunauer, S., *J. Amer. Chem. Soc.* **64**, 745 (1942).
18. Klemm, R., *U. S. Dept. Comm. Office Tech. Serv. P. B. Rept.* **82**, 353.
19. Uchida, H., and Todo, N., *Bull. Chem. Soc. Jap.* **29**, 20 (1956).
20. Hall, W. K., Tarn, W. H., and Anderson, R. B., *J. Amer. Chem. Soc.* **72**, 5436 (1950).
21. Bulstuikova, Yu, I., Apel'baum, L. O., and Temkin, M. I., *Zh. Fiz. Khim.* **32**, 2717 (1958).
22. Kamzolkin, V. P., and Avdeeva, A. V., *Zh. Khim. Prom.* **10**, 32 (1933).
23. Shultz, J. F., Hofer, L. J. E., Karn, F. S., and Anderson, R. B., *J. Phys. Chem.* **66**, 501 (1962).
24. Freel, J., Pieters, W. J. M., and Anderson, R. B., *J. Catal.* **16**, 281 (1970).
25. Kempling, J. C., and Anderson, R. B., *Ind. Eng. Chem., Process Des. Develop.* **9**, 116 (1970).
26. Satterfield, C. N., *Ind. Eng. Chem.* **61**, 4 (1969).
27. Bell, R. P., *J. Chem. Soc.* (London) 1371 (1931).
28. Emmett, P. H., *in* "Advances in Catalysis" (W. G. Frankenburg, V. I. Komarewsky, and E. K. Rideal, Eds.), Vol. 1, p. 65. Academic Press, New York.